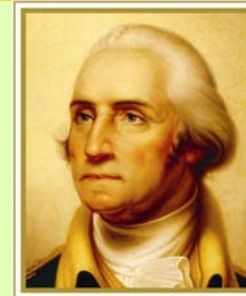
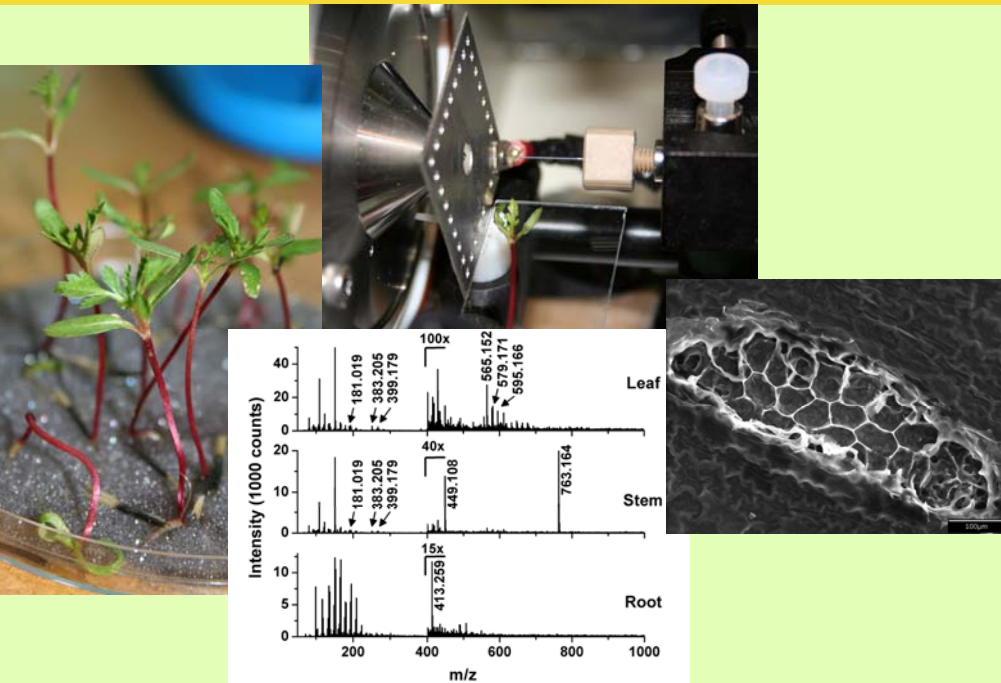


Atmospheric Pressure Laser Ablation Ion Sources for Biomolecules and Synthetic Polymers

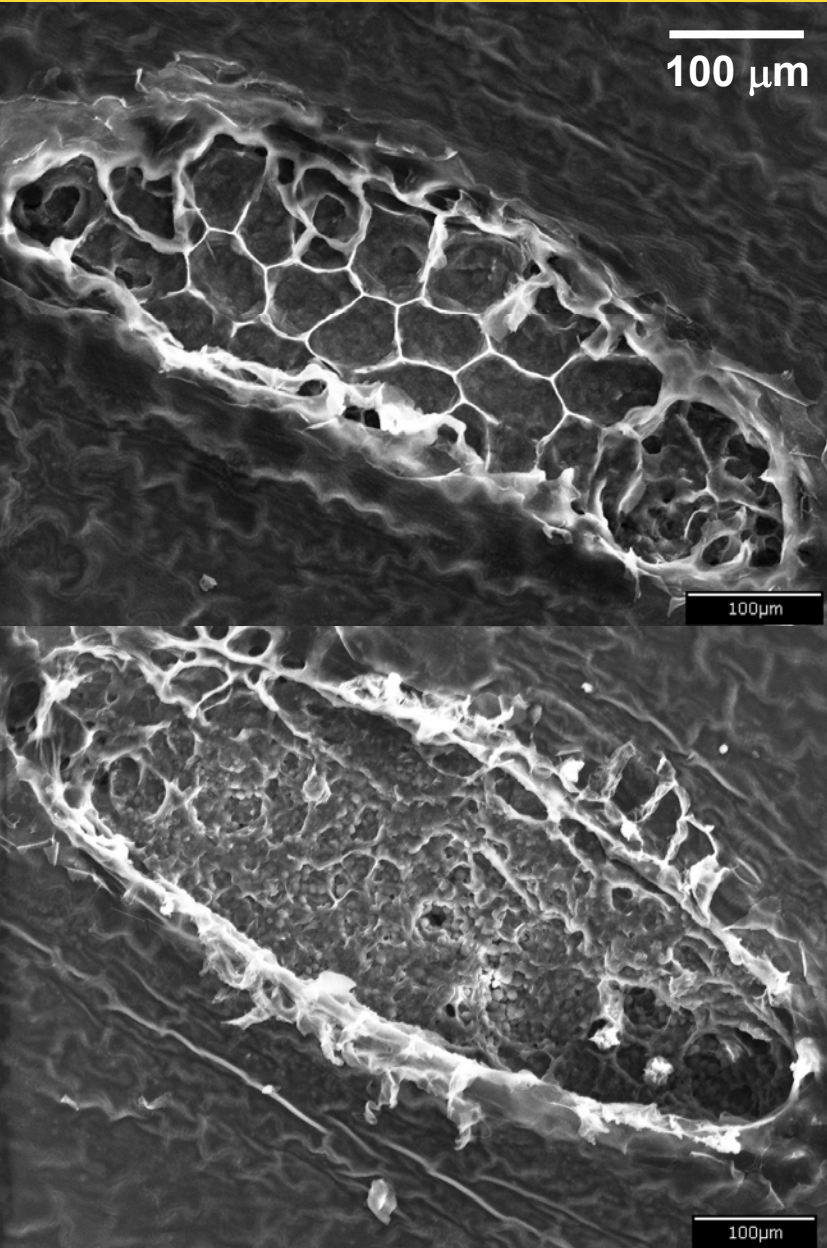


THE GEORGE
WASHINGTON
UNIVERSITY
WASHINGTON DC

DEPARTMENT OF CHEMISTRY

Akos Vertes, Peter Nemes,
Bindesh Shrestha, Alexis A. Barton,
Zhaoyang Chen and Yue Li

In vivo biochemical analysis



Laser ablation of soft tissue:

- surgery, nanosurgery
- transfection
- elemental analysis
- biochemical analysis

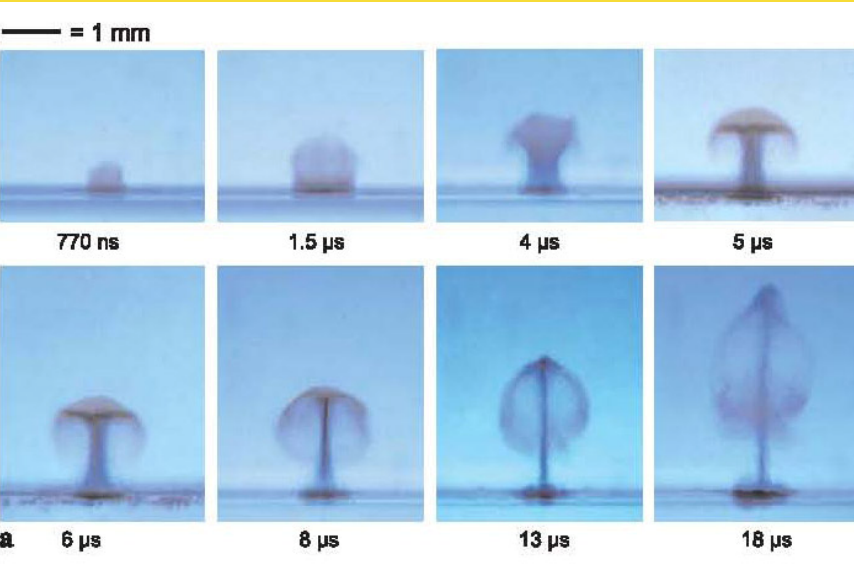
Obstacles for *in vivo* observations with mass spec:

- vacuum conditions
- denaturing matrixes in MALDI

Objectives:

- explore plume dynamics
- MS imaging at atmospheric pressure with no matrix
- 3D chemical imaging

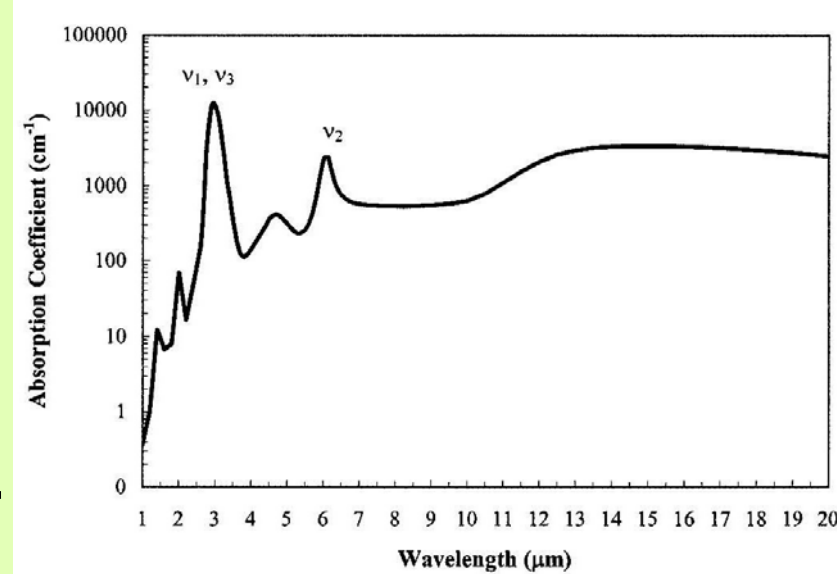
Mid-IR laser ablation of water



Apitz and Vogel, *Appl. Phys. A*, 2005, 81, 329.

Three phases of ablation:

- Surface evaporation
- Phase explosion
- Fluid ejection



Specific for water:

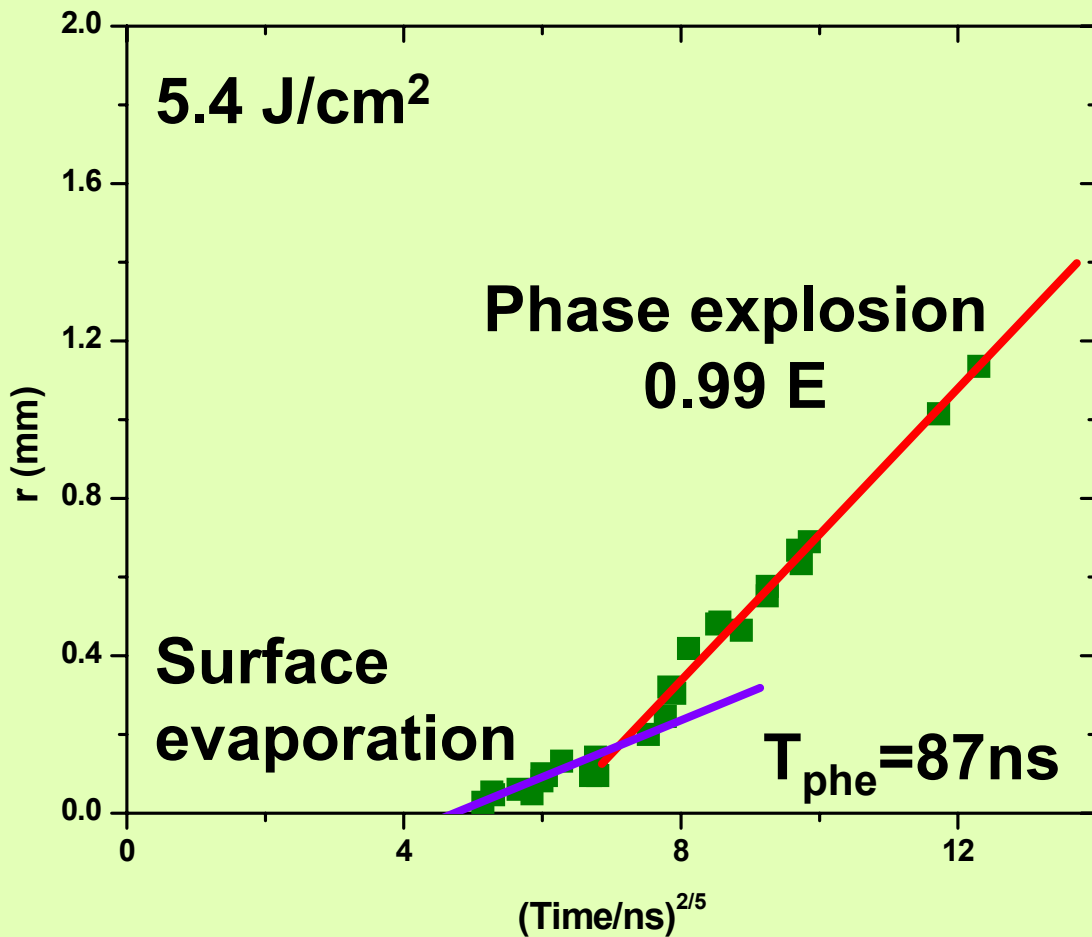
- **Surface evaporation vs. phase explosion**
- **Non-linear absorption (at high T → transparent)**

Shori et al., *IEEE J. Select. Top. Quant. Electr.*, 2001, 7, 959.

Similarity modeling: Taylor

Er:YAG laser, 2.94 μm , water

■ I. Apitz and A. Vogel, *SPIE*, **4961** (2003) 48.

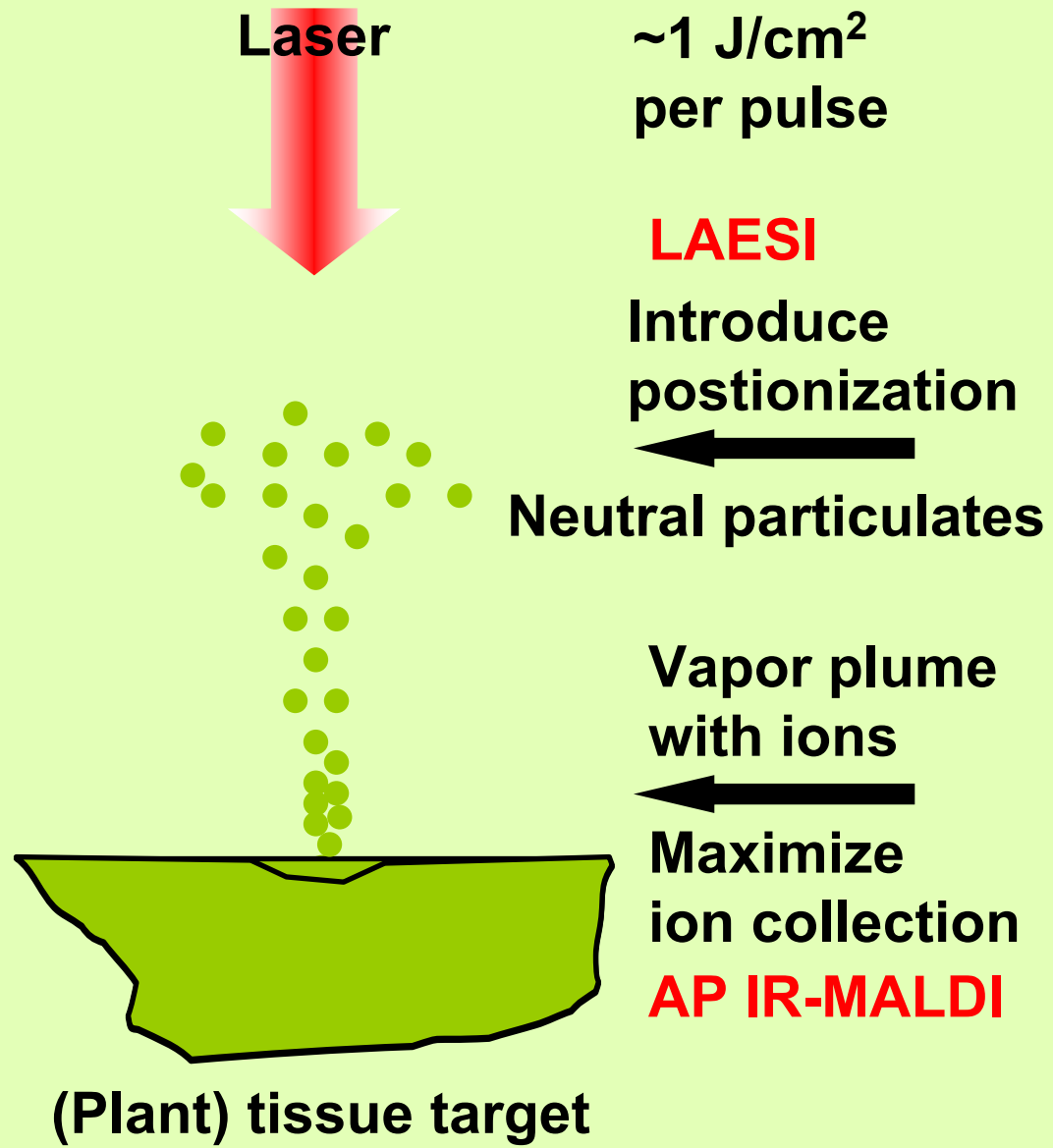
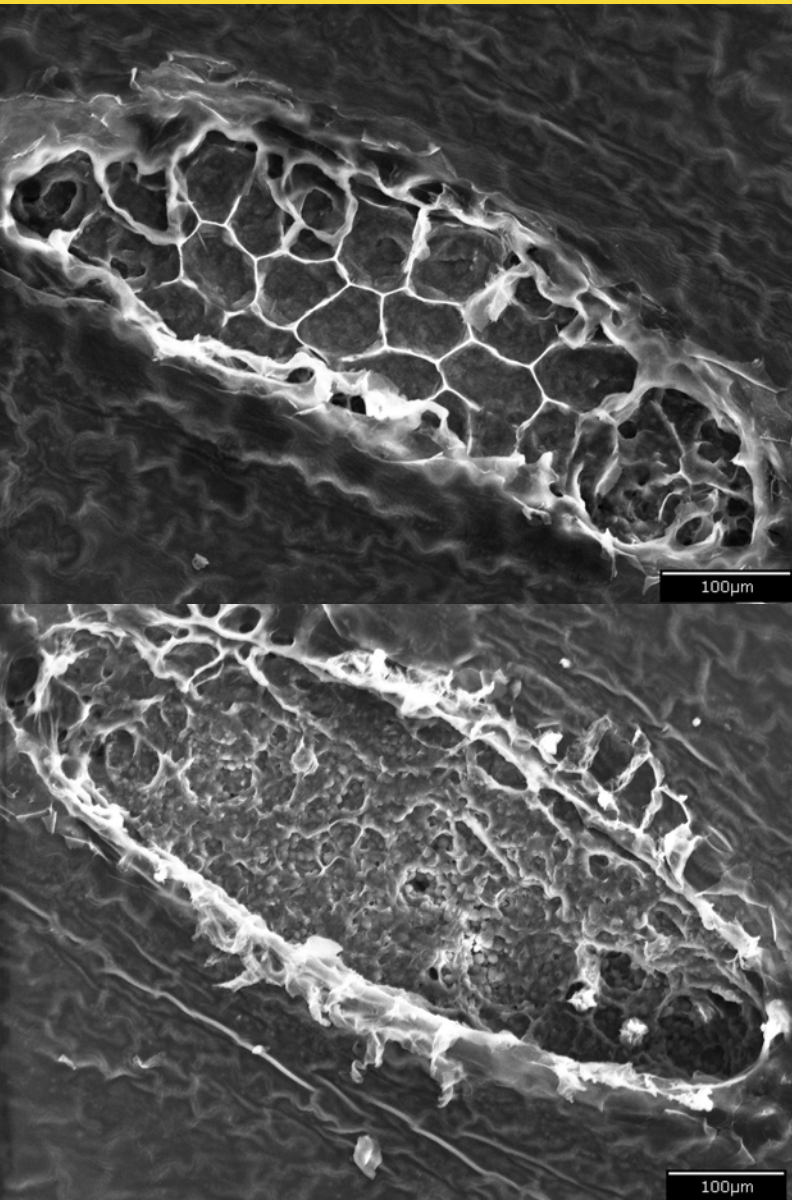


Plume front position

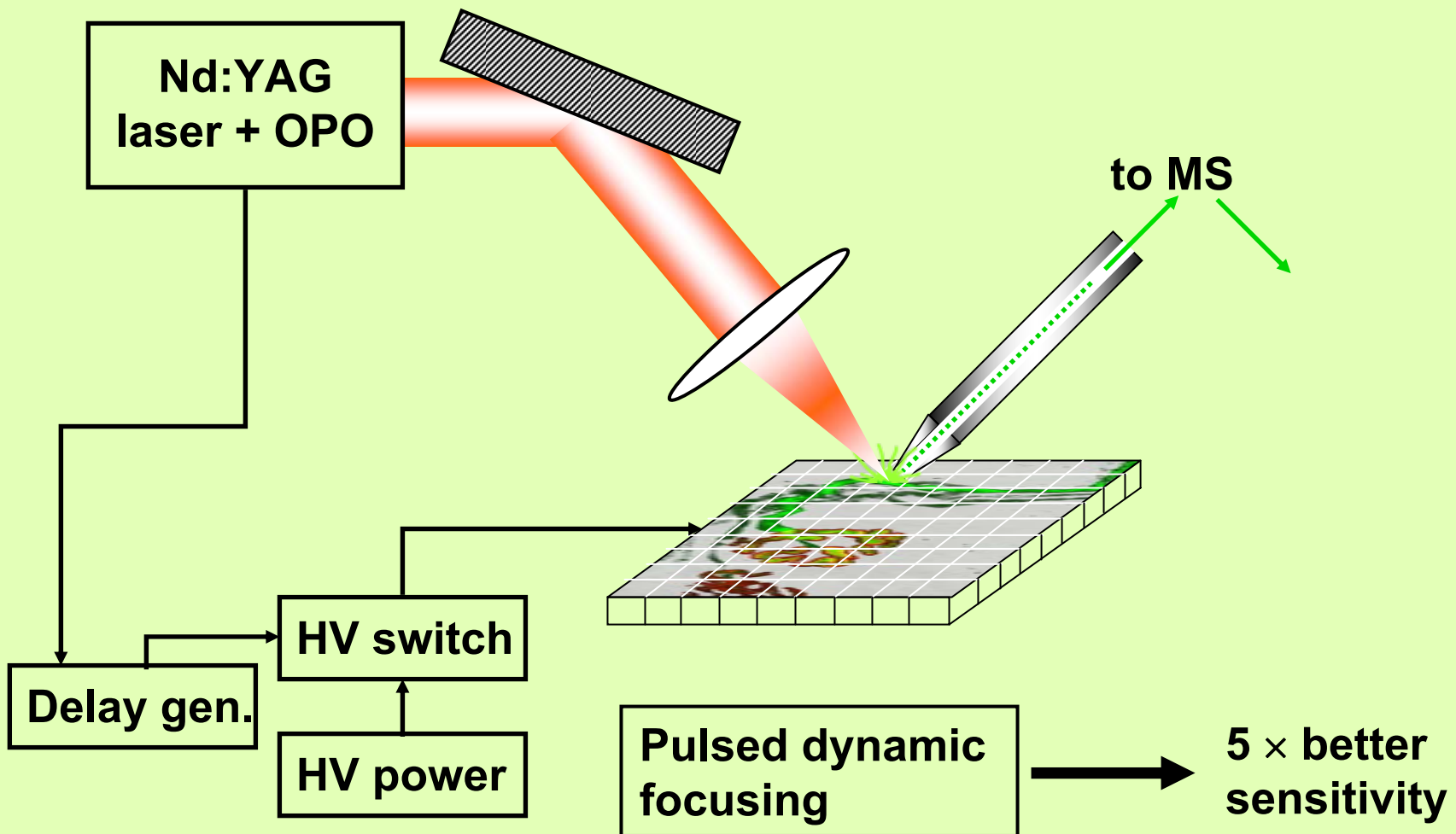
Taylor, *Proc. Roy. Soc. London A*, 1950, **201**, 159.

$$r = S(\gamma) E^{\frac{1}{5}} \rho_0^{-\frac{1}{5}} t^{\frac{2}{5}}$$

Mid-IR laser ablation of tissues

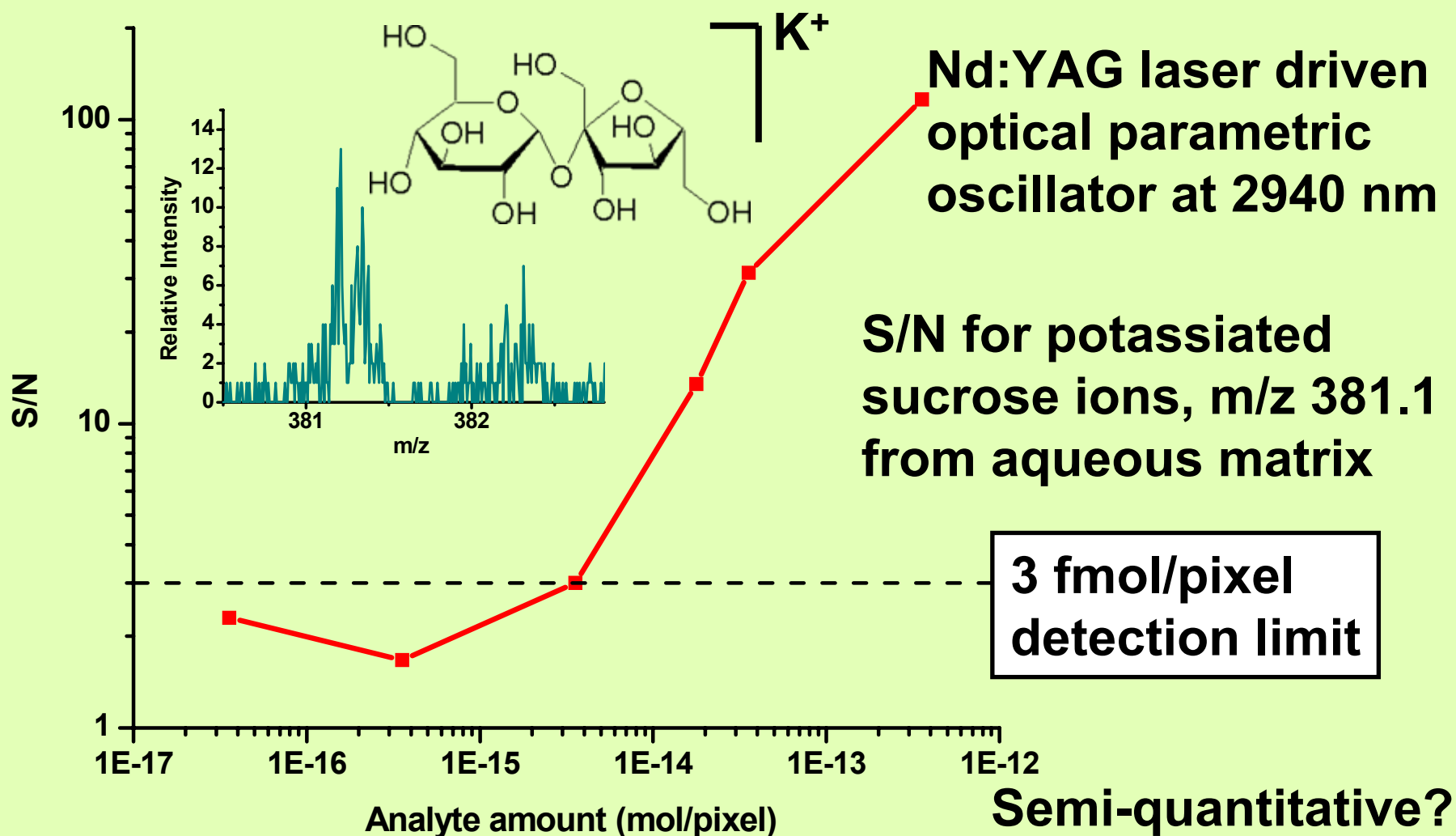


AP IR-MALDI imaging with PDF



AP IR-MALDI detection limit

Pulsed dynamic focusing (PDF)



Spatial resolution

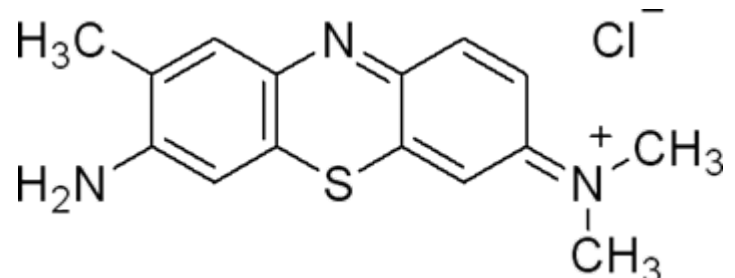
AP IR-MALDI

R ap-maldi grids

060402_AP_1A 3774 (69.259) Cm (3774:3789)

100

100



%

206.7775

204.7751

256.0820

254.0702

271.1018

272.0973

284.1107

286.6992

306.7126

366.6313

383.6370

402.6451

446.5583

464.5677

467.5574

527.4944544.4884

601.1074

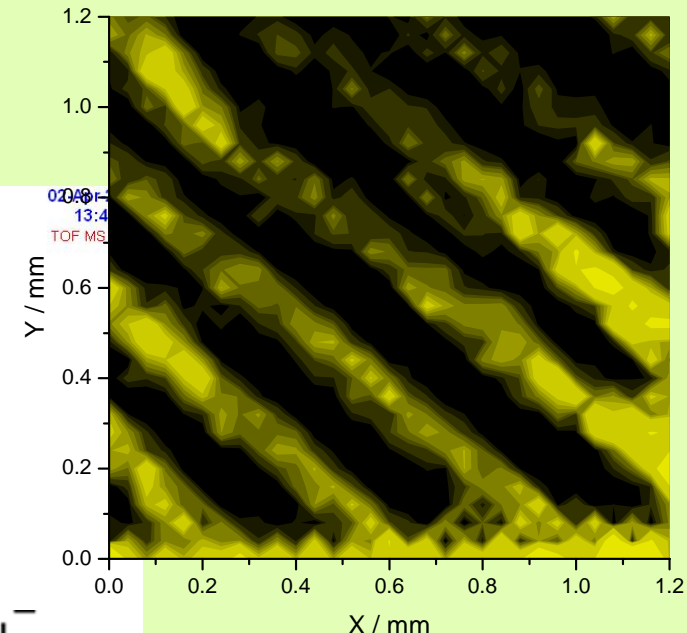
603.1138

606.4108

639.4090

m/z

Toluidine blue O
Masked with grid
Gap width 92 μm

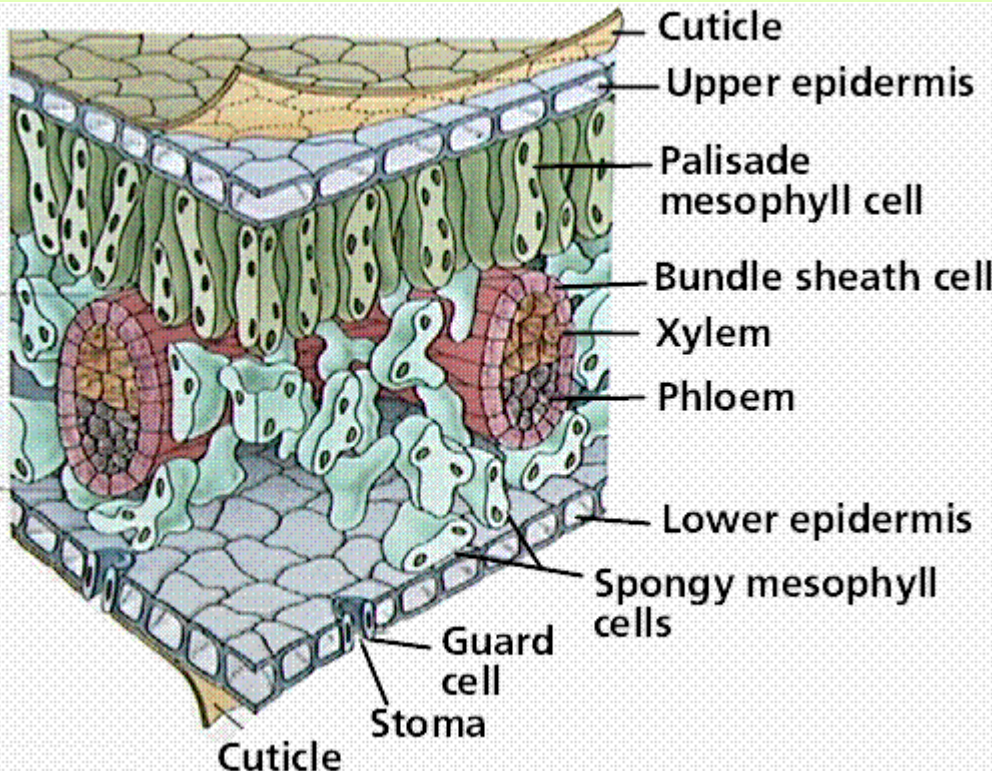


0.048 H
13:4
TOF MS

Oversampling:
40 μm resolution

Plant organs - leaf

AP IR-MALDI: Cilantro – *Coriandrum sativum*



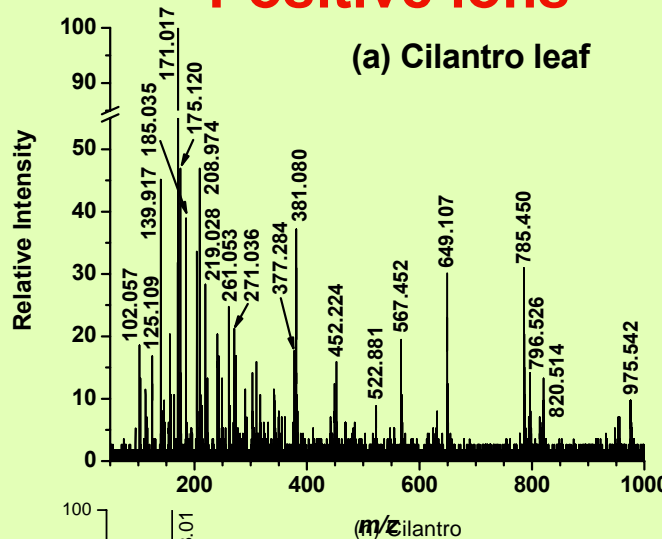
Vein

<http://www.emc.maricopa.edu/faculty/farabee/biobk/BioBookPLANTANAT.html>

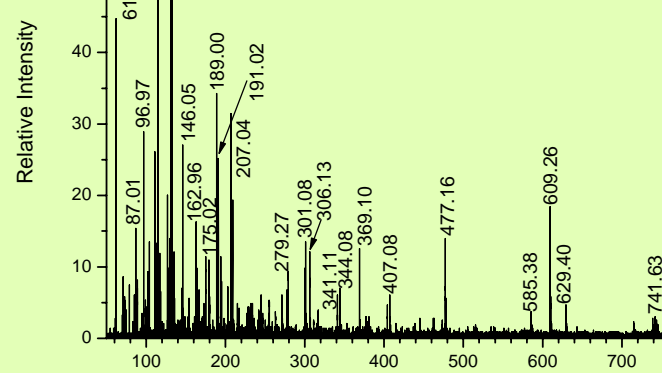
- >50 metabolites
- Numerous metabolic pathways
- ~10 mDa mass accuracy

Positive ions

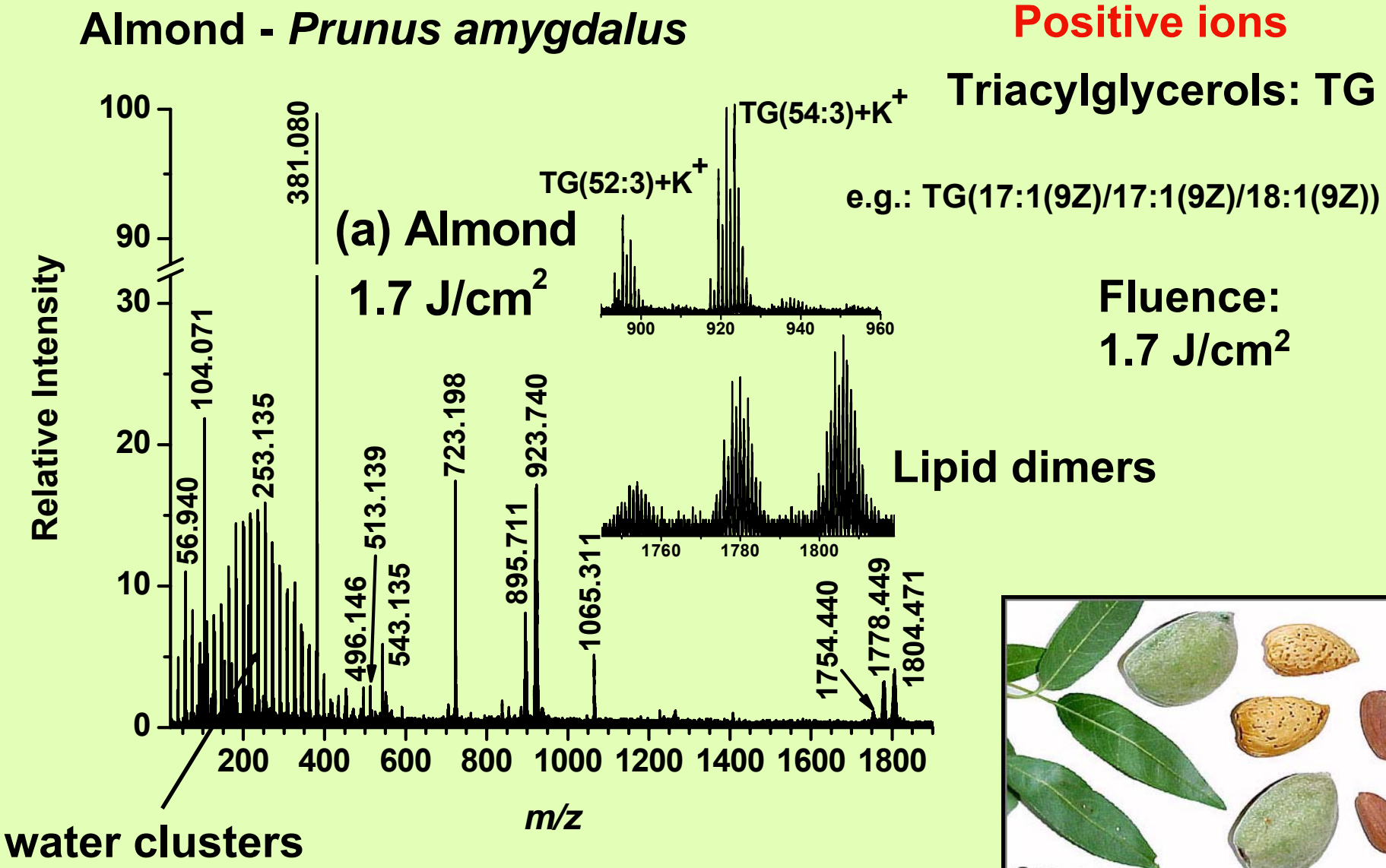
(a) Cilantro leaf



Negative ions

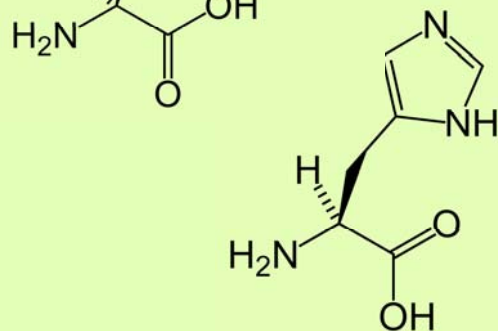
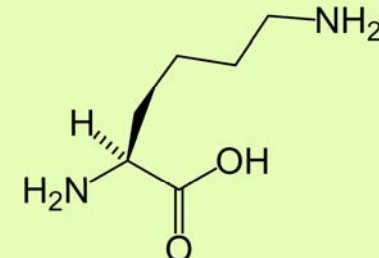
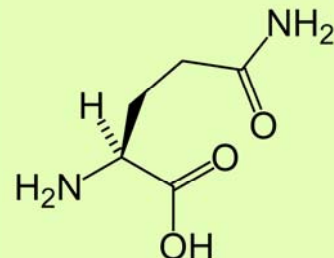
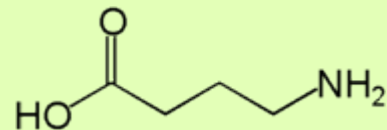


Plant organs - seeds

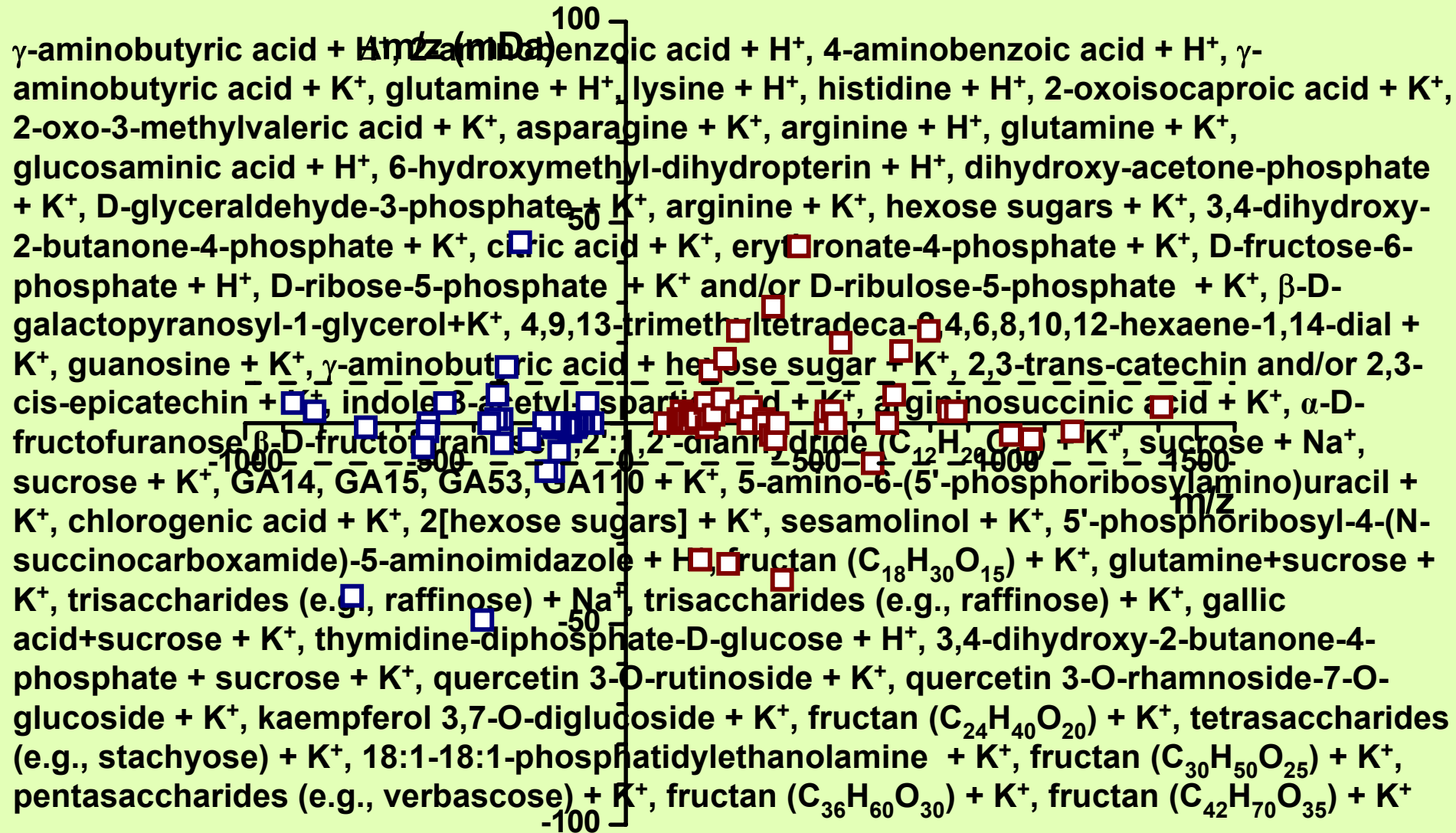


Ions from plant tissue

Observed m/z	Exact m/z	$\Delta m/z (10^{-3})$	Ion	Plant organs ^a	Metabolic pathways ^b
104.071 ^c	104.0711	0	γ -aminobutyric acid + H ⁺	BU, FL, FR, SE, TU	arginine degradation, glutamate degradation
138.056	138.0555	+1	2-aminobenzoic acid + H ⁺	FR	tryptophan biosynthesis
			4-aminobenzoic acid + H ⁺	FR	tetrahydrofolate biosynthesis
142.027 ^c	142.0270	0	γ -aminobutyric acid + K ⁺	FR, TU	arginine degradation, glutamate degradation
147.080	147.0770	+3	glutamine + H ⁺	FR	arginine, asparagine, histidine and tryptophan biosynthesis, <i>de novo</i> biosynthesis of purine nucleotides
147.114	147.1134	+1	lysine + H ⁺	BU	lysine biosynthesis and degradation and methionine salvage pathway
156.078	156.0773	+1	histidine + H ⁺	FR	histidine biosynthesis and methionine salvage pathway



Mass accuracy of assignments



Identified from plant tissue

Over 50 small metabolites including:

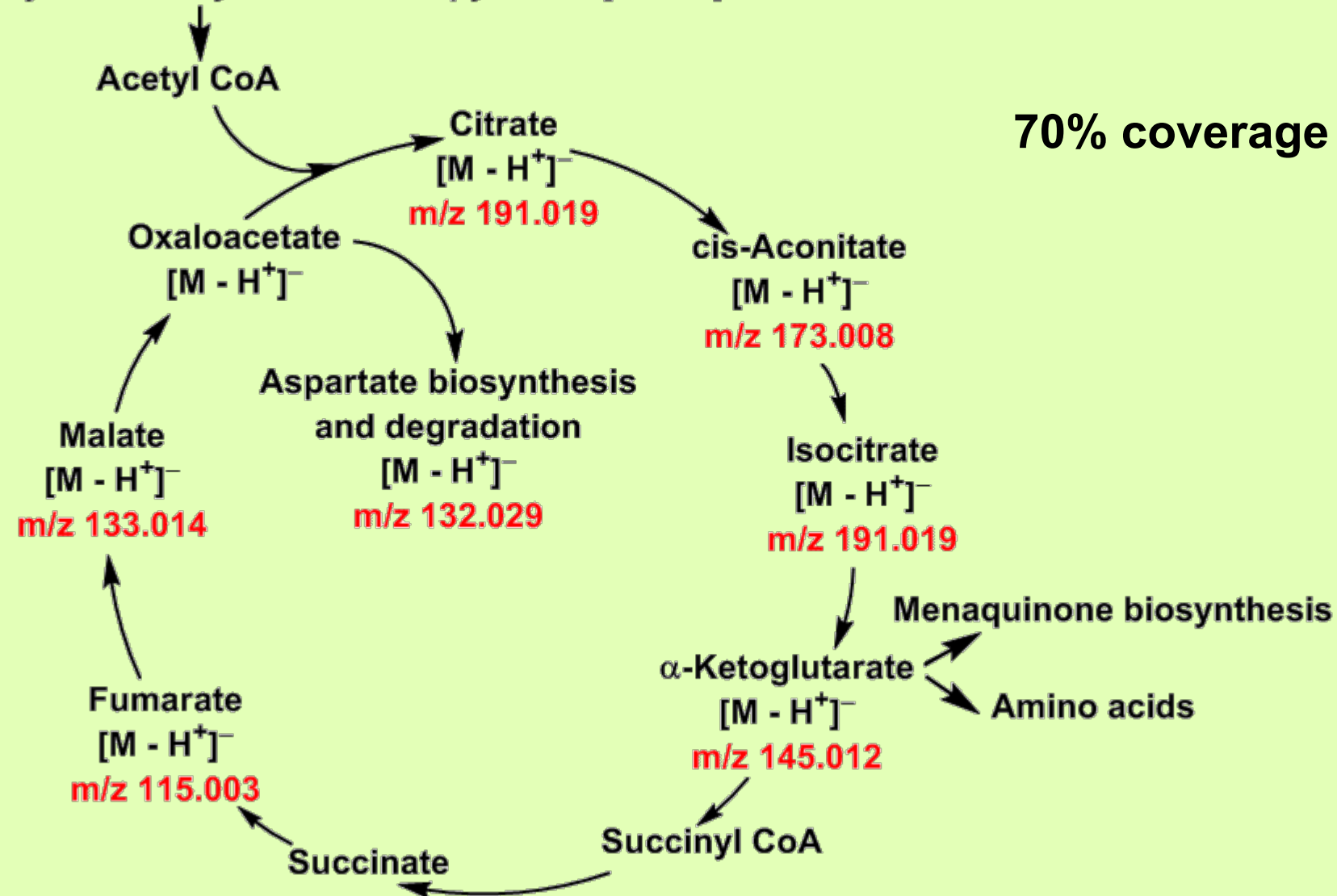
- carbohydrates and oligosaccharide synthesis
- amino acids
- organic acids
- lipids
- miscellaneous metabolites

Metabolic pathways:

- glycolysis pathway
- phospholipid biosynthesis
- reactants and/or products of amino acid biosynthesis
- nucleotide biosynthesis
- oligosaccharide biosynthesis
- flavonoid biosynthesis

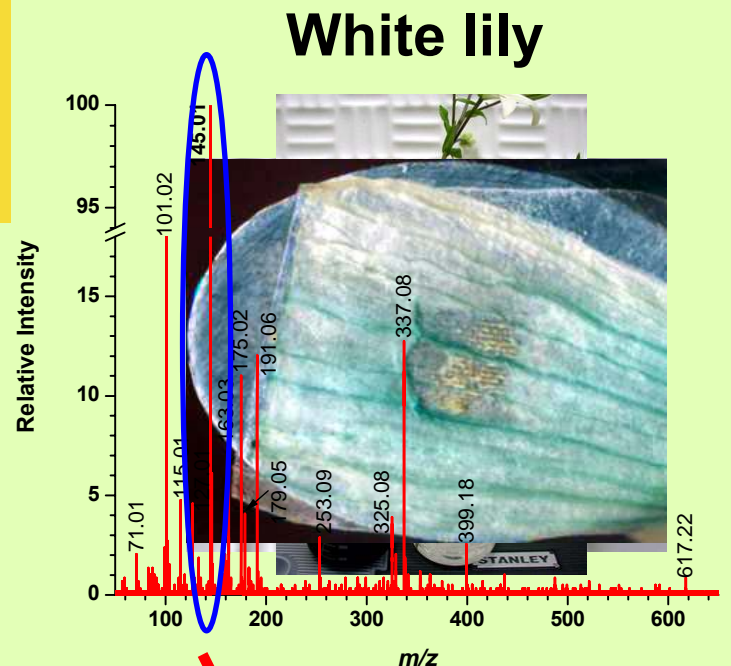
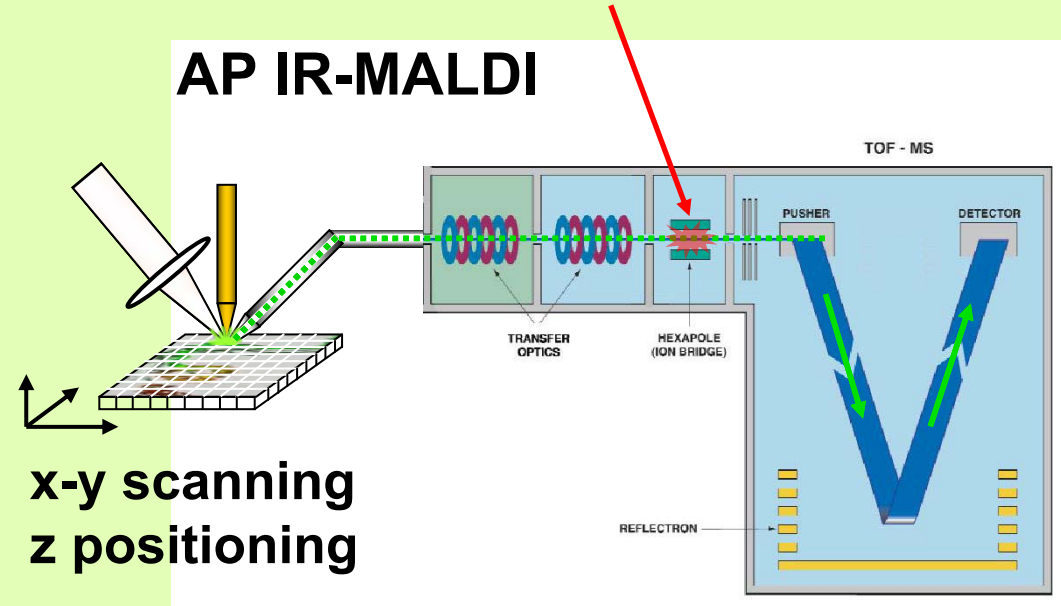
Citric acid cycle - respiration

acetyl CoA biosynthesis from pyruvate $[M - H^+]^-$ m/z 87.008

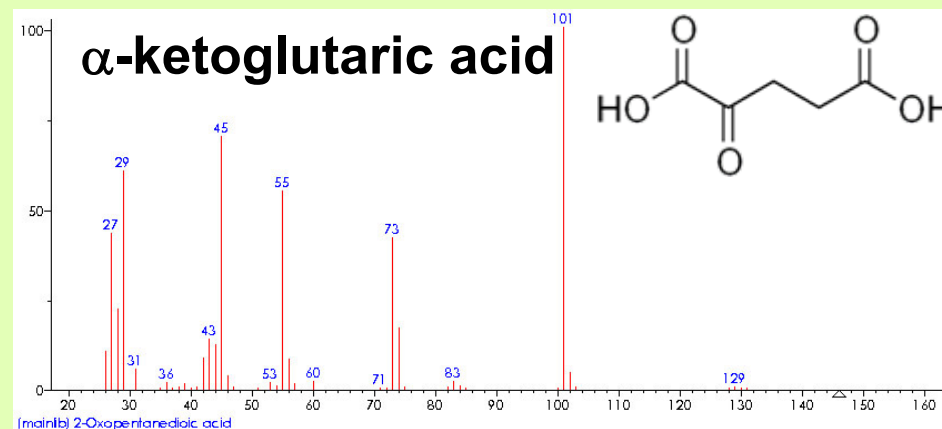


Plant transpiration

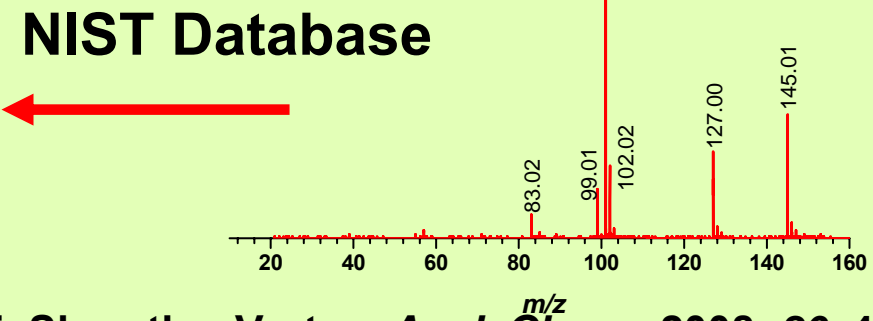
Collision activated dissociation



CAD - m/z 145.01

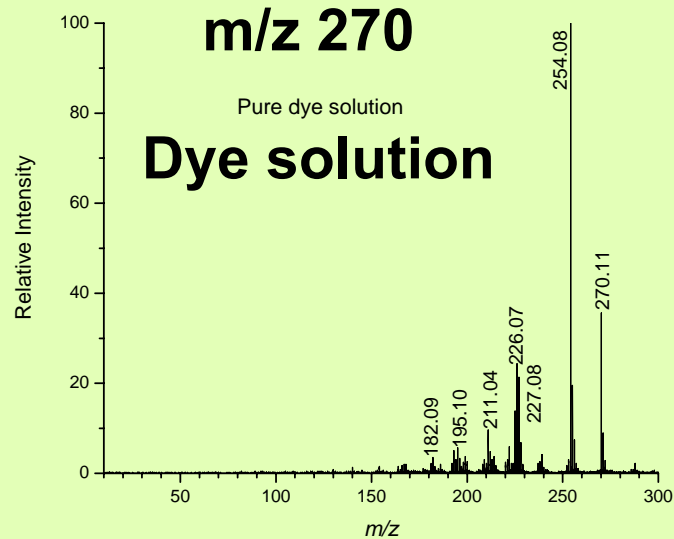
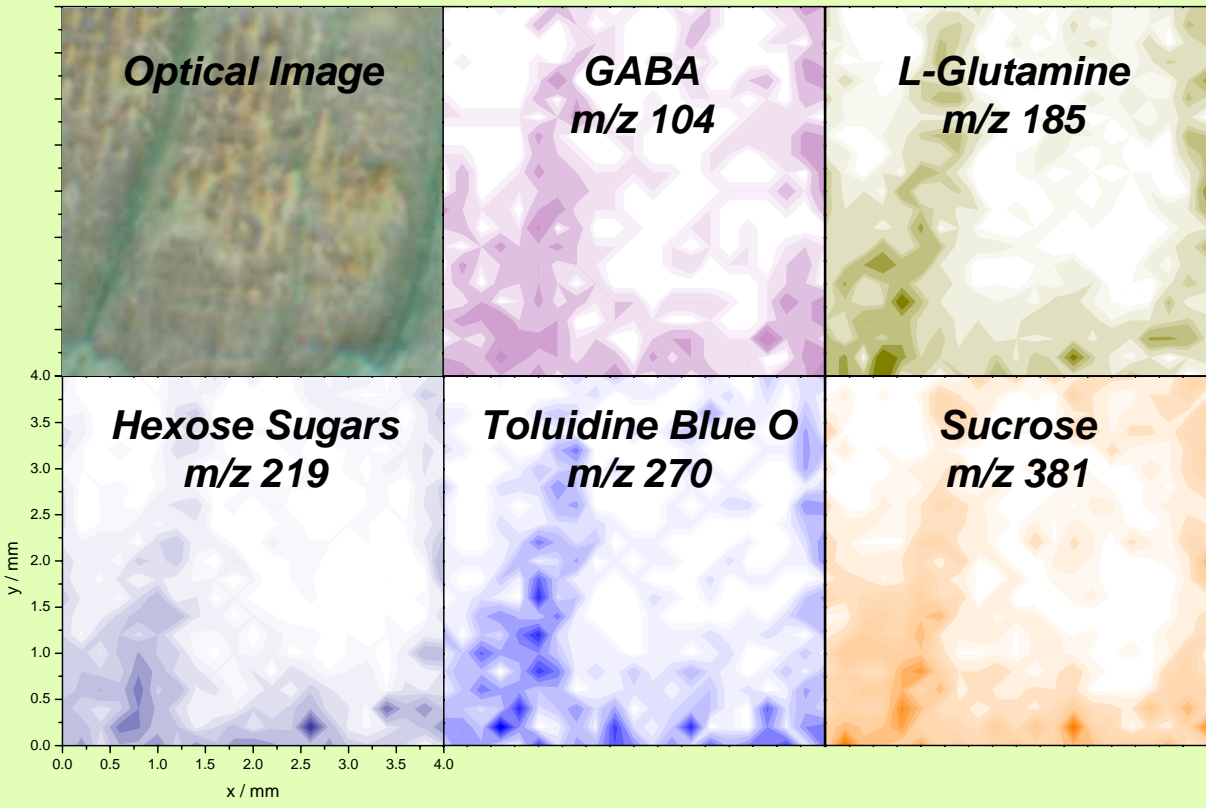


NIST Database

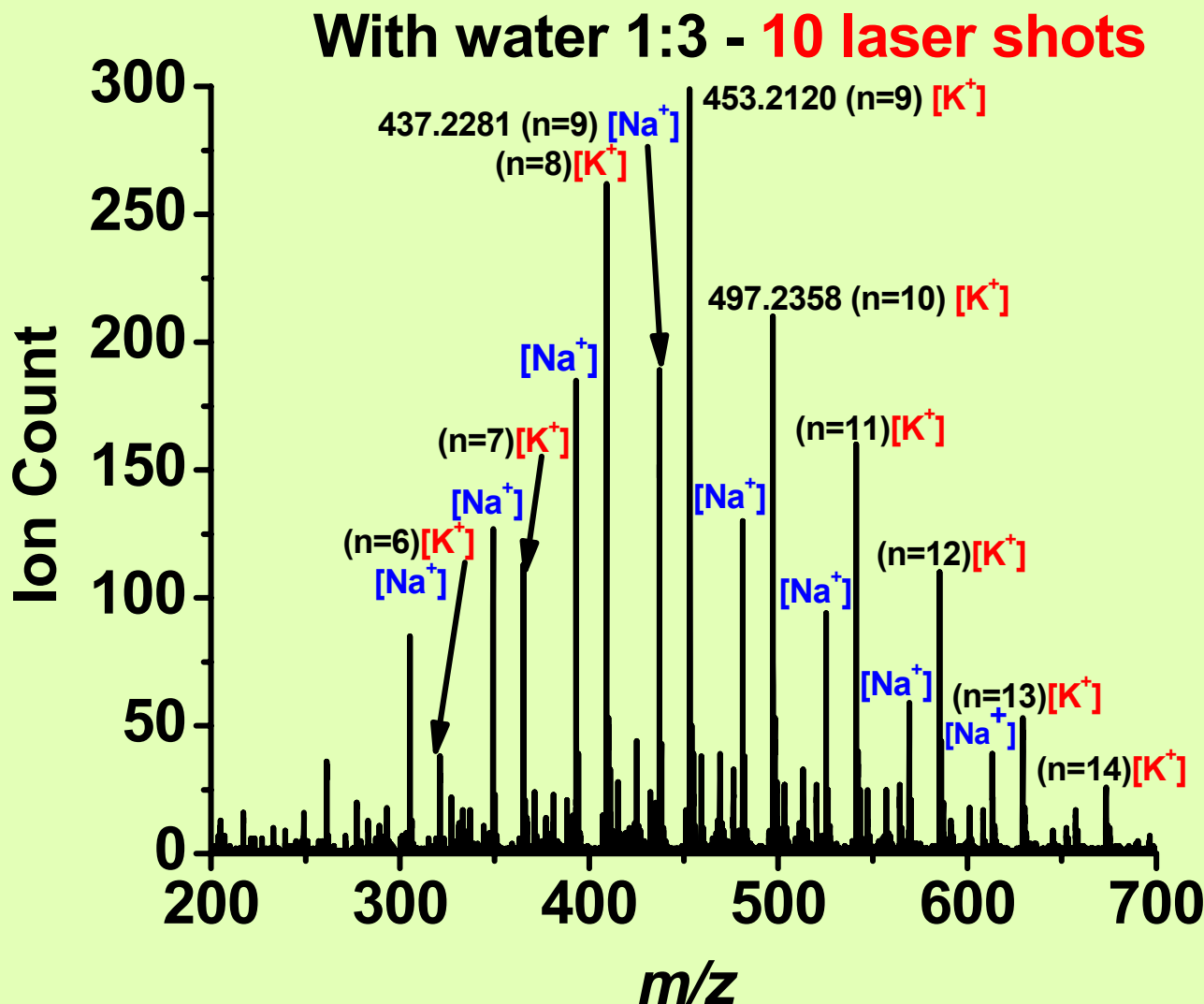


Li, Shrestha, Vertes, *Anal. Chem.*, 2008, 80, 407.

Plant transpiration

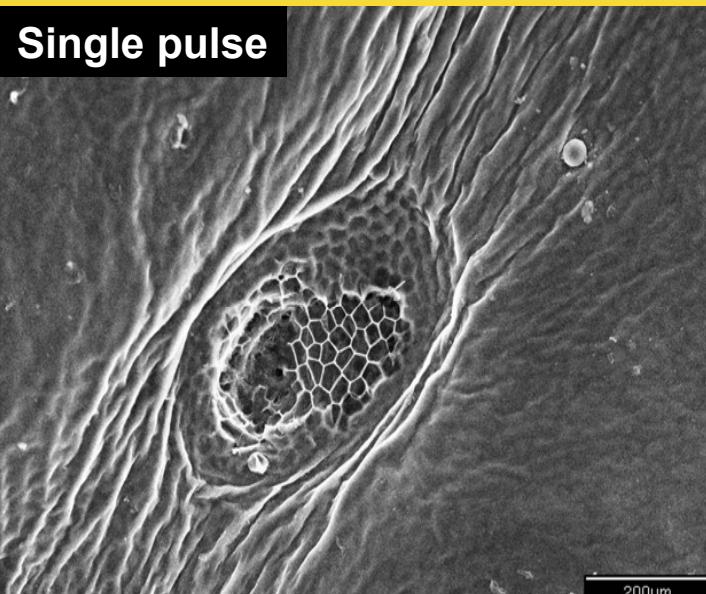


AP IR-MALDI of PEG M_n 570-630

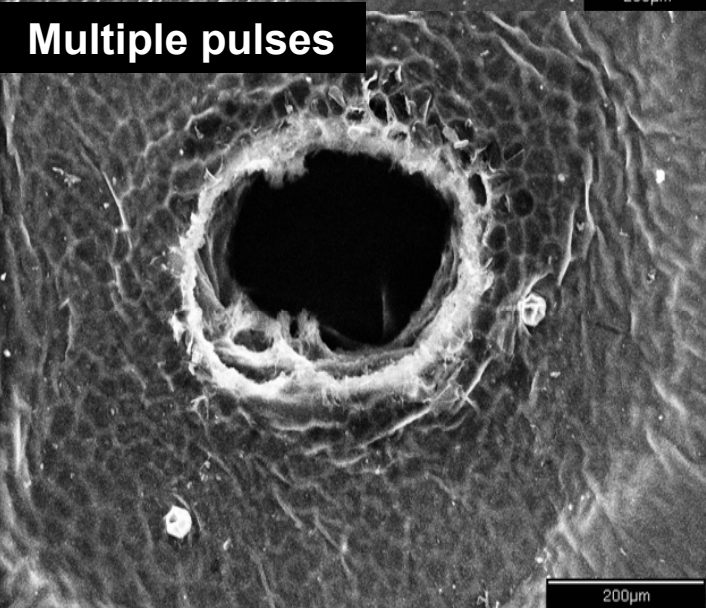


Mid-IR laser ablation of tissues

Single pulse



Multiple pulses



Laser



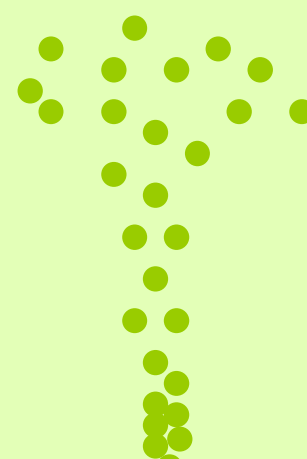
$\sim 1 \text{ J/cm}^2$
per pulse

LAESI

Introduce
positionization



Neutral particulates



Vapor plume
with ions

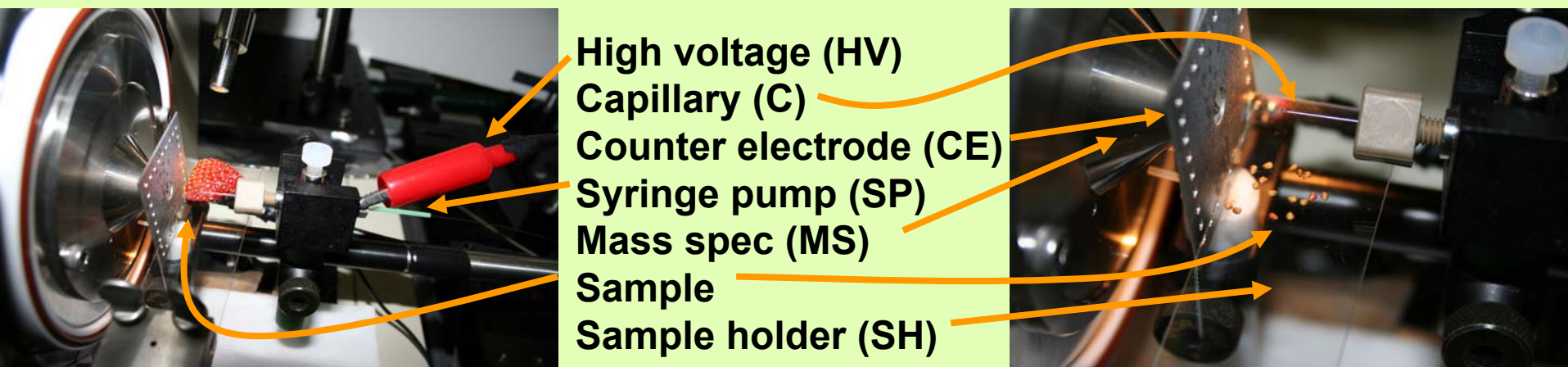
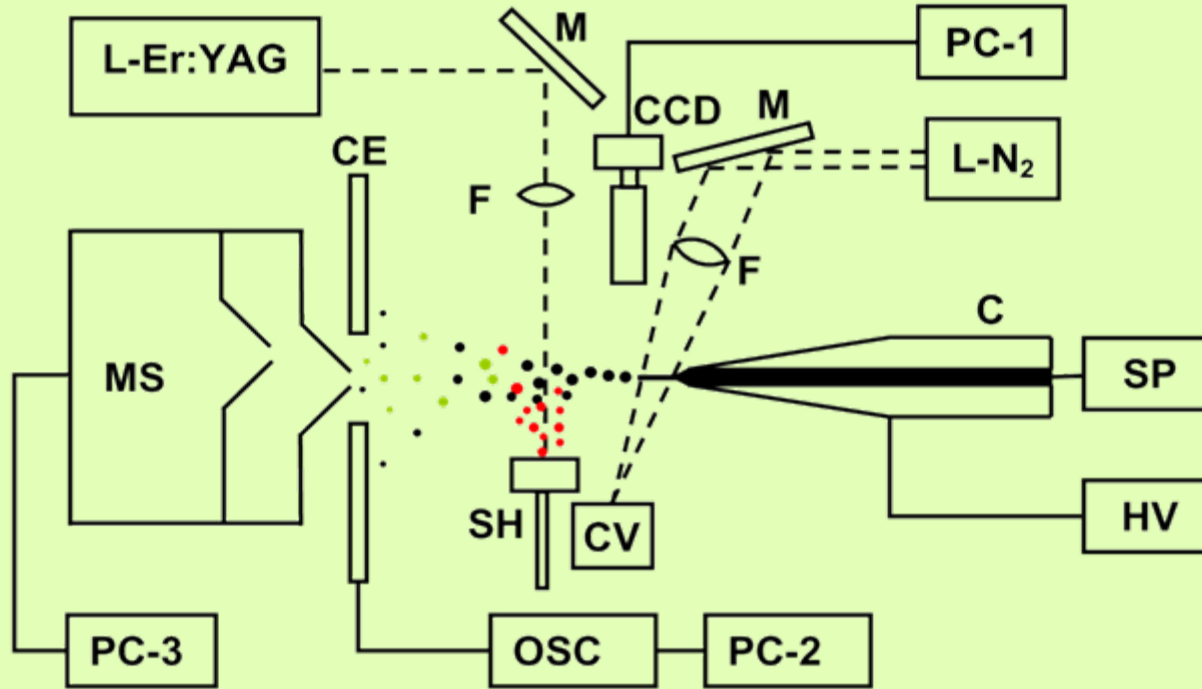


Maximize
ion collection

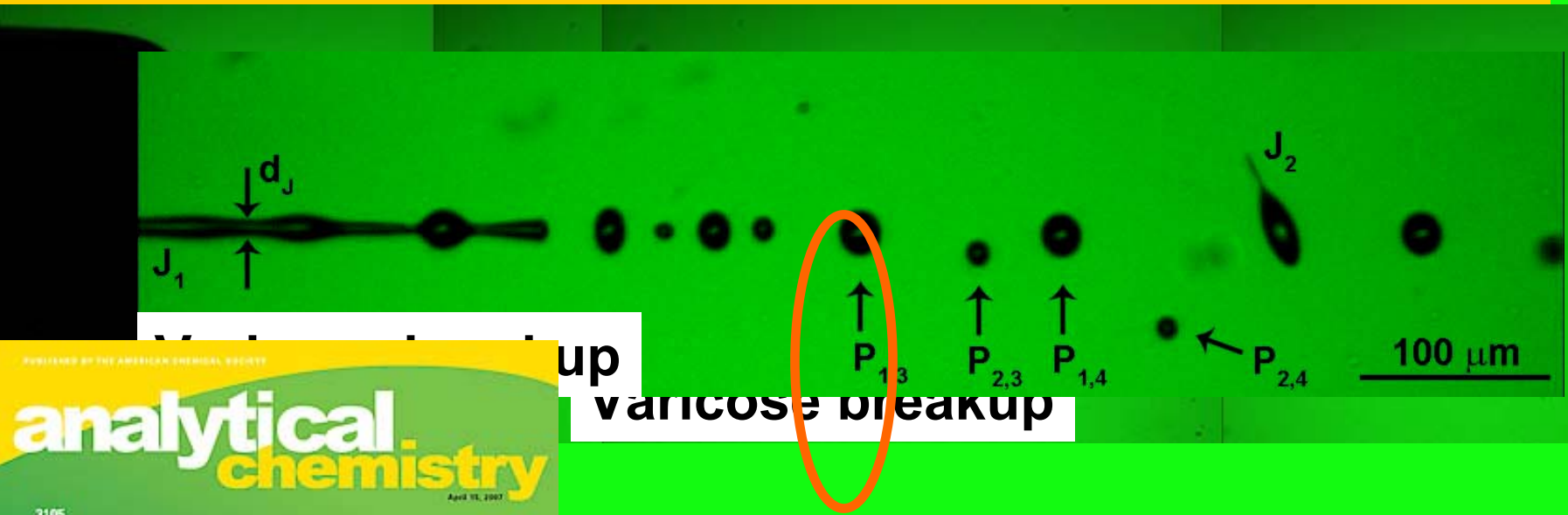
AP IR-MALDI

(Plant) tissue target

Laser ablation electrospray ionization (LAESI)

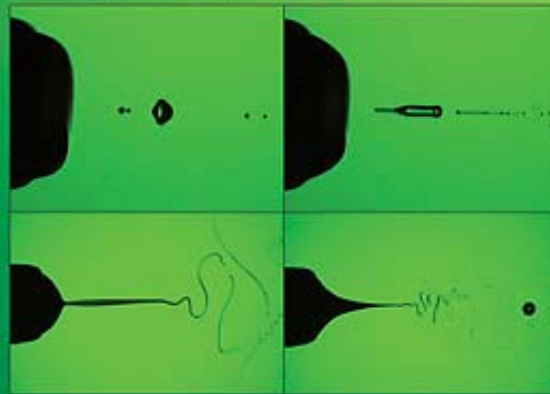


Droplet formation and fission in ESI



JOURNAL OF THE AMERICAN CHEMICAL SOCIETY
analytical chemistry

3105
Spraying Mode Effect on Droplet Formation and Ion Chemistry in Electrosprays



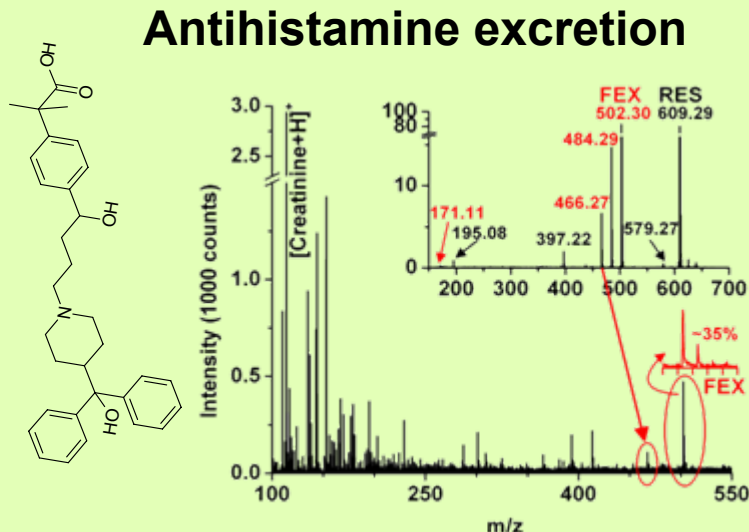
3041
Online Concentration and Affinity Separation of Biomolecules Using Multifunctional Particles in CE under Magnetic Field

3091
Comprehensive 2D FFF/LC in the Analysis of Large Molecules

Lateral kink breakup

LAESI MS capabilities

From small drug molecules to large biomolecules:

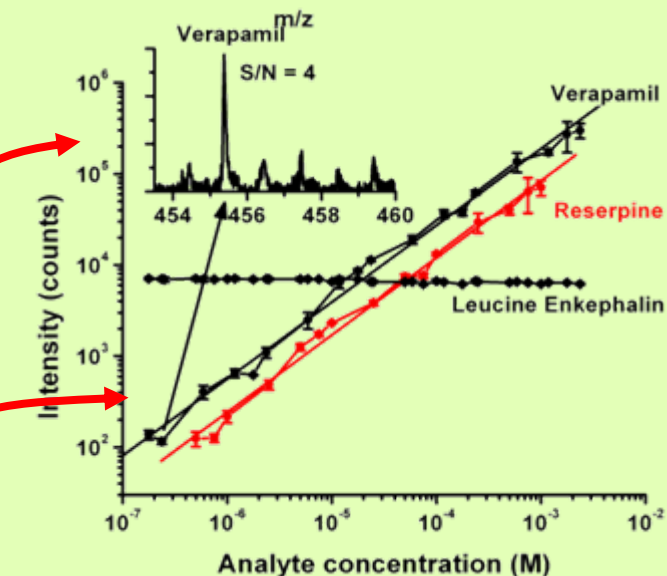
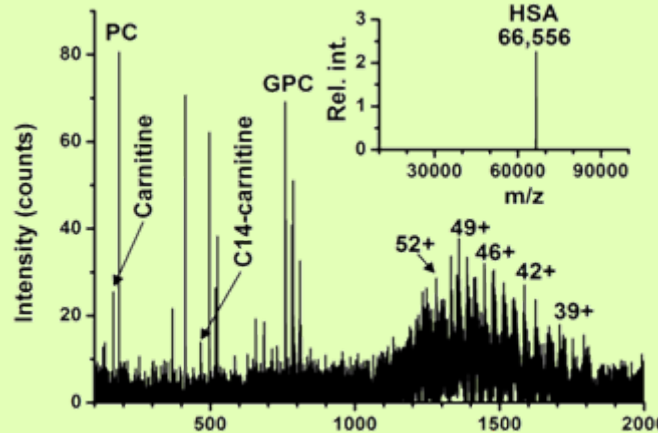


Fexofenadine (FEX), the active component of Allegra, detected directly from urine 2 hours after administration caplet.

Limit of detection: 8 fmol for verapamil

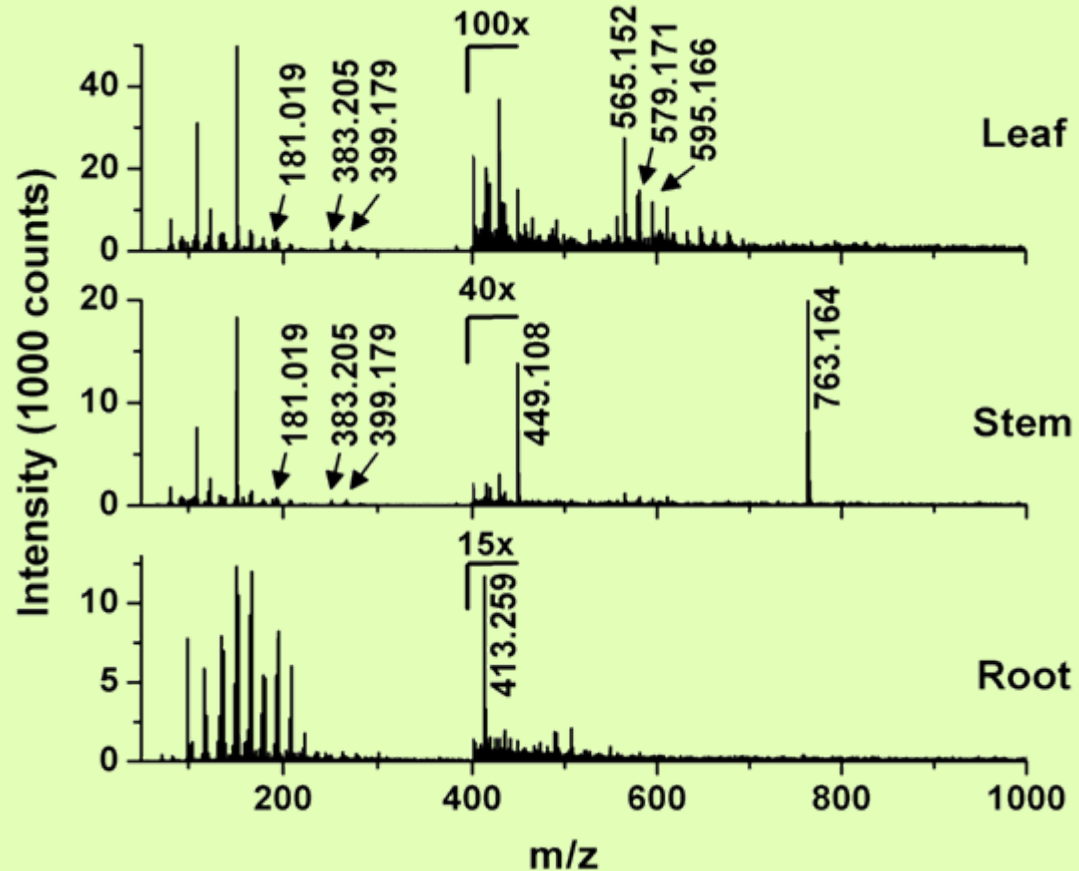
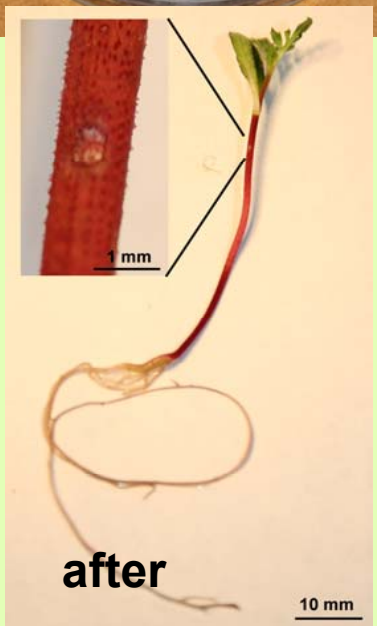
Quantitation: 4-decade dynamic range

Human serum albumin in serum



LAESI for in vivo spatial profiling

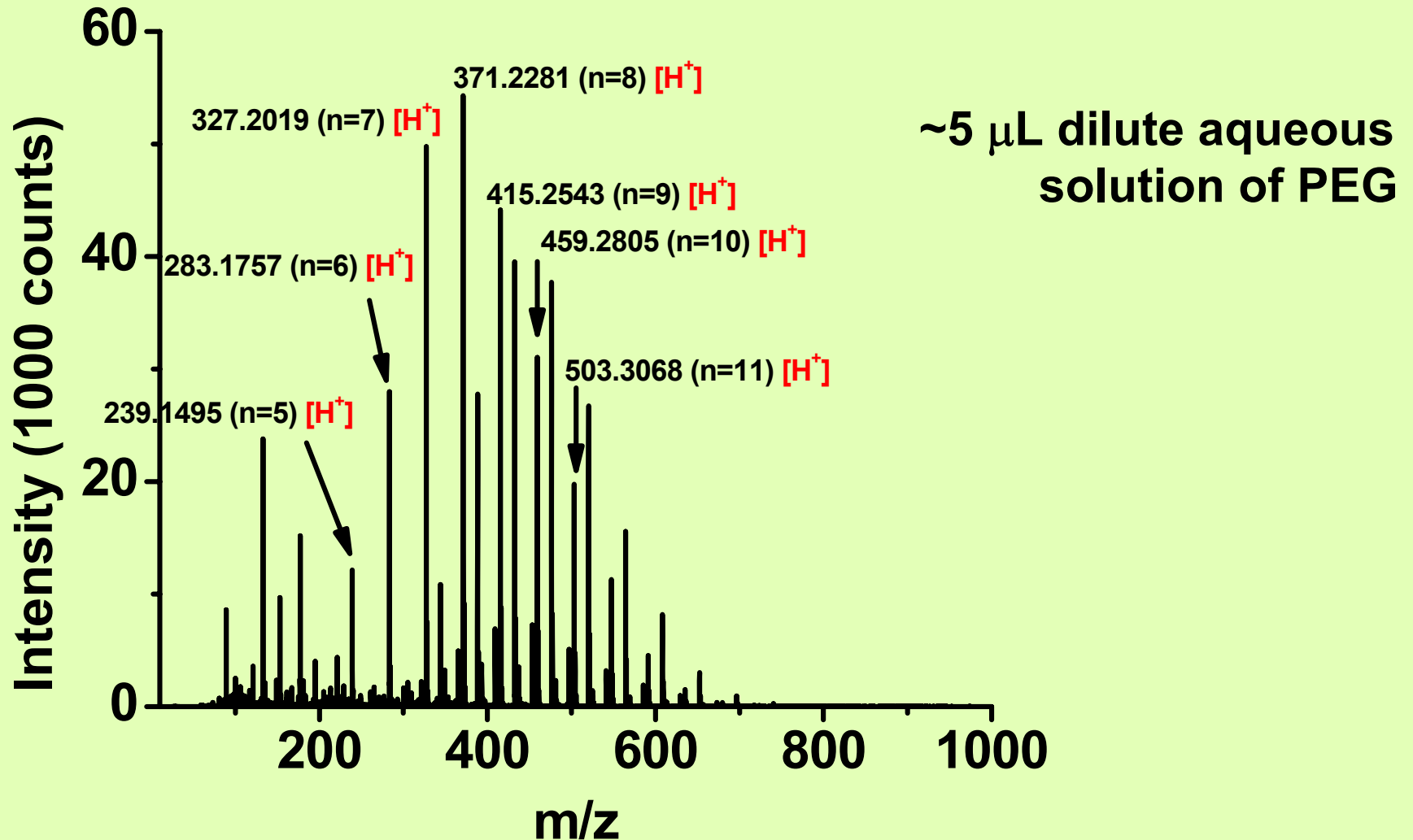
LAESI profiling of 1-week old French marigold (*Tagetes Patula*) seedlings



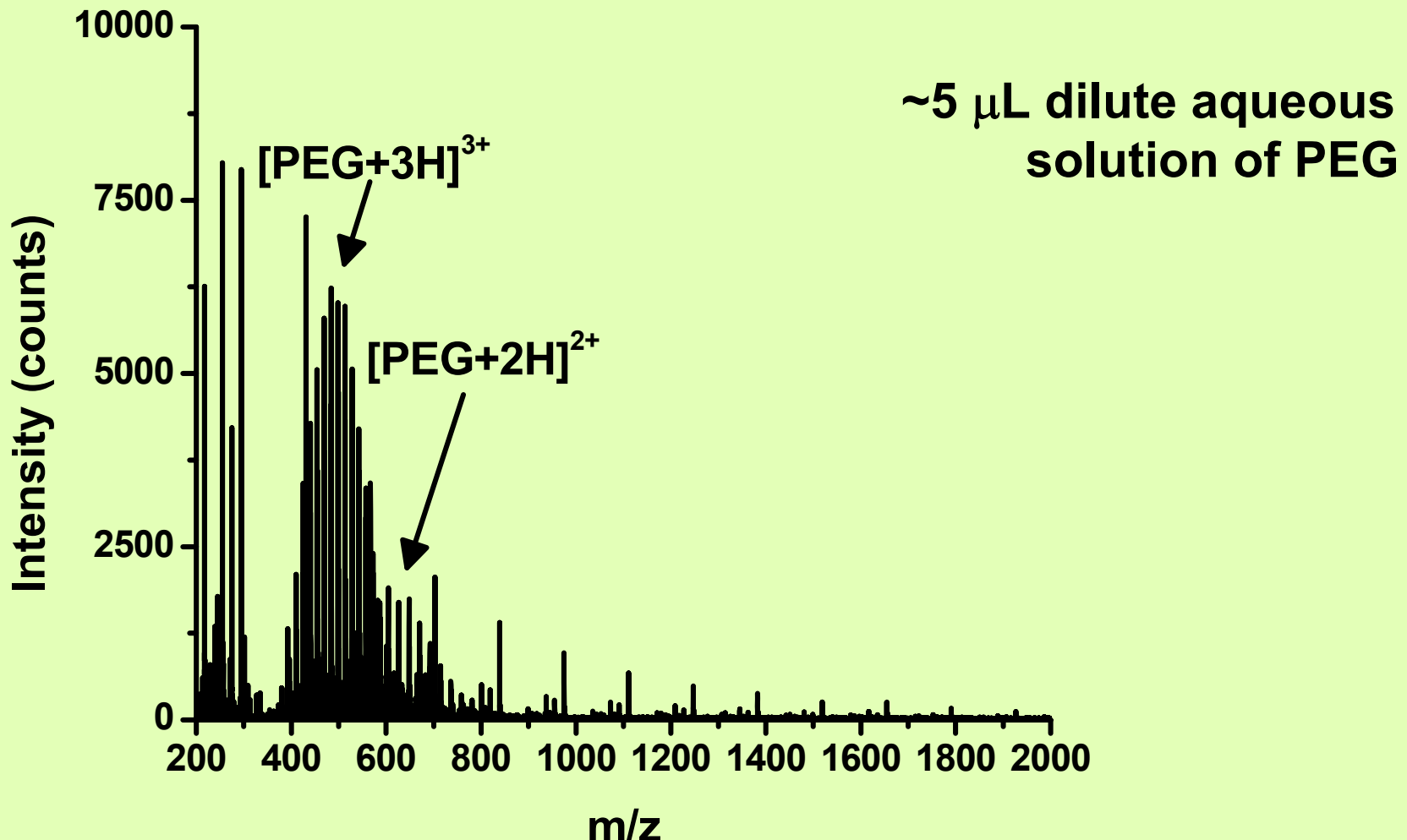
Organ-specific chemicals detected *in vivo*, e.g.:

- kaempferol dirhamnoside (m/z 579.1) in leaf
- cyanidin glucoside m/z 449.1) in stem
- methylsalicylate (m/z 154.0) in root

LAESI of PEG-400

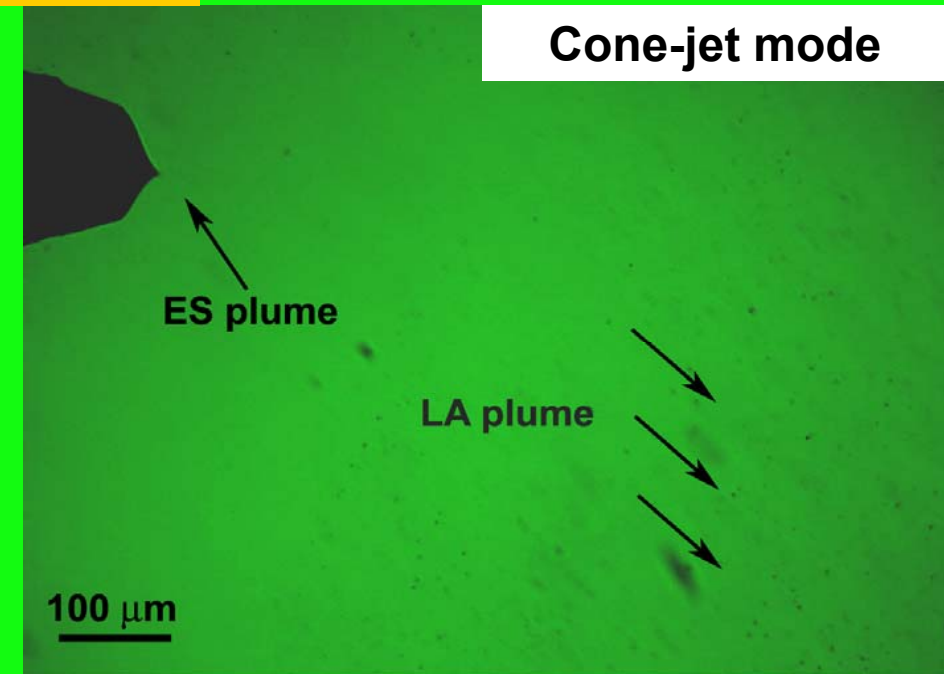
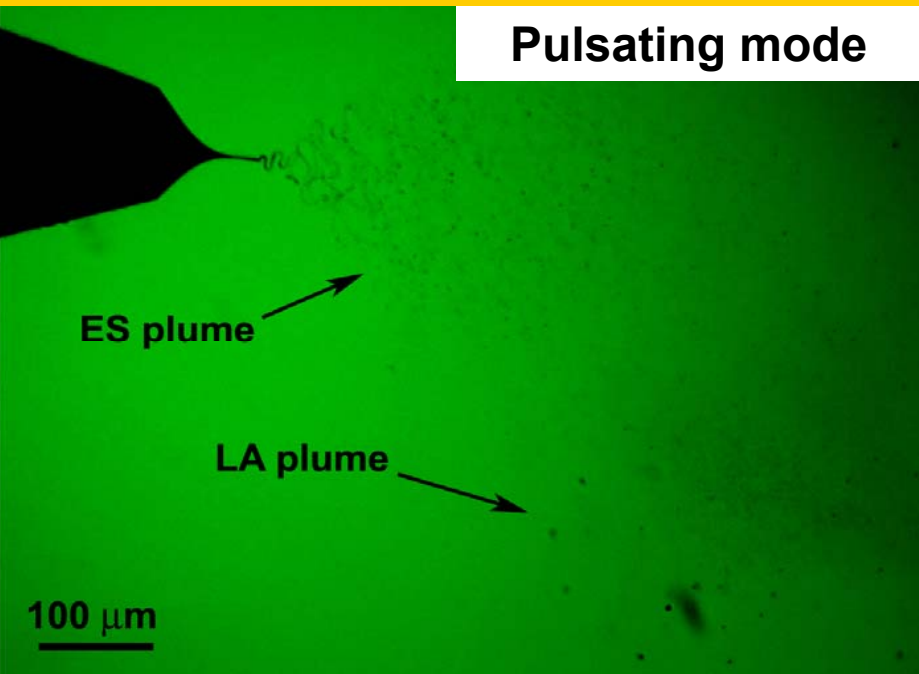


LAESI of PEG-1500



LAESI mechanism

Fast (7 ns) imaging of LAESI
with 50% ethanol



LAESI mechanism:

- Electrospray operating in (preferably) cone-jet mode → critically charged droplets
- Infrared laser ablation of target → LA plume of neutrals (particulates, nanoparticles, clusters, etc.) produced
- Intersection of LA plume and spray → neutrals engulfed by spray droplets
- Electrospray ionization follows → multiply charged ions generated

LAESI molecular imaging



Zebra plant
(*Aphelandra Squarrosa*)

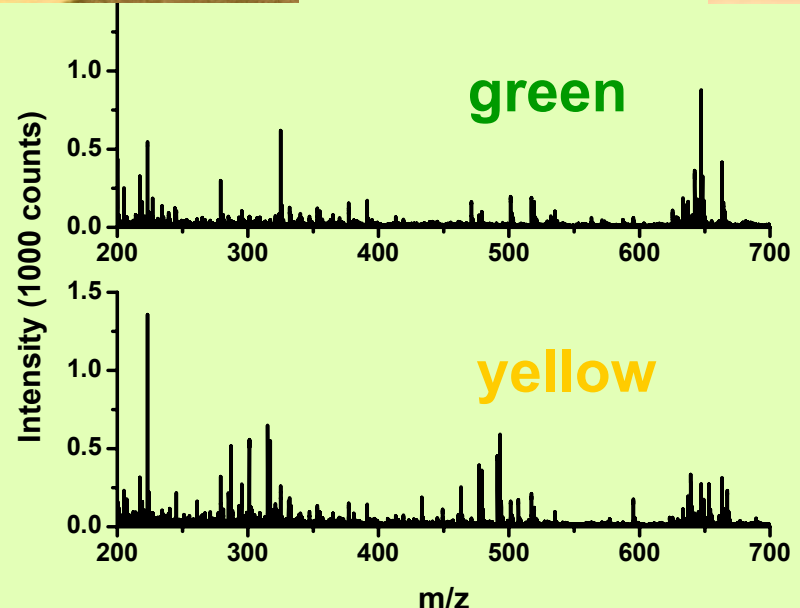
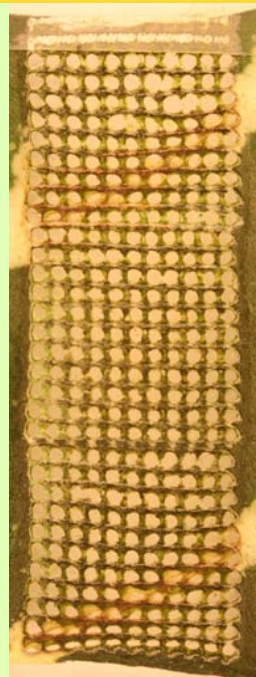
Yellow sectors contain cyanidin, luteolinidin compounds, e.g., cyanidin-hexoside (m/z 449.10)



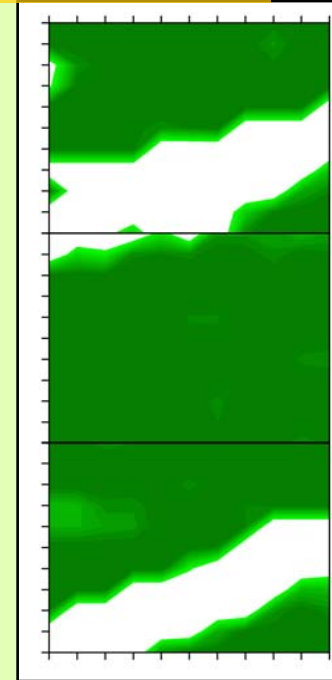
Variegated leaf

Surface rastered with laser beam

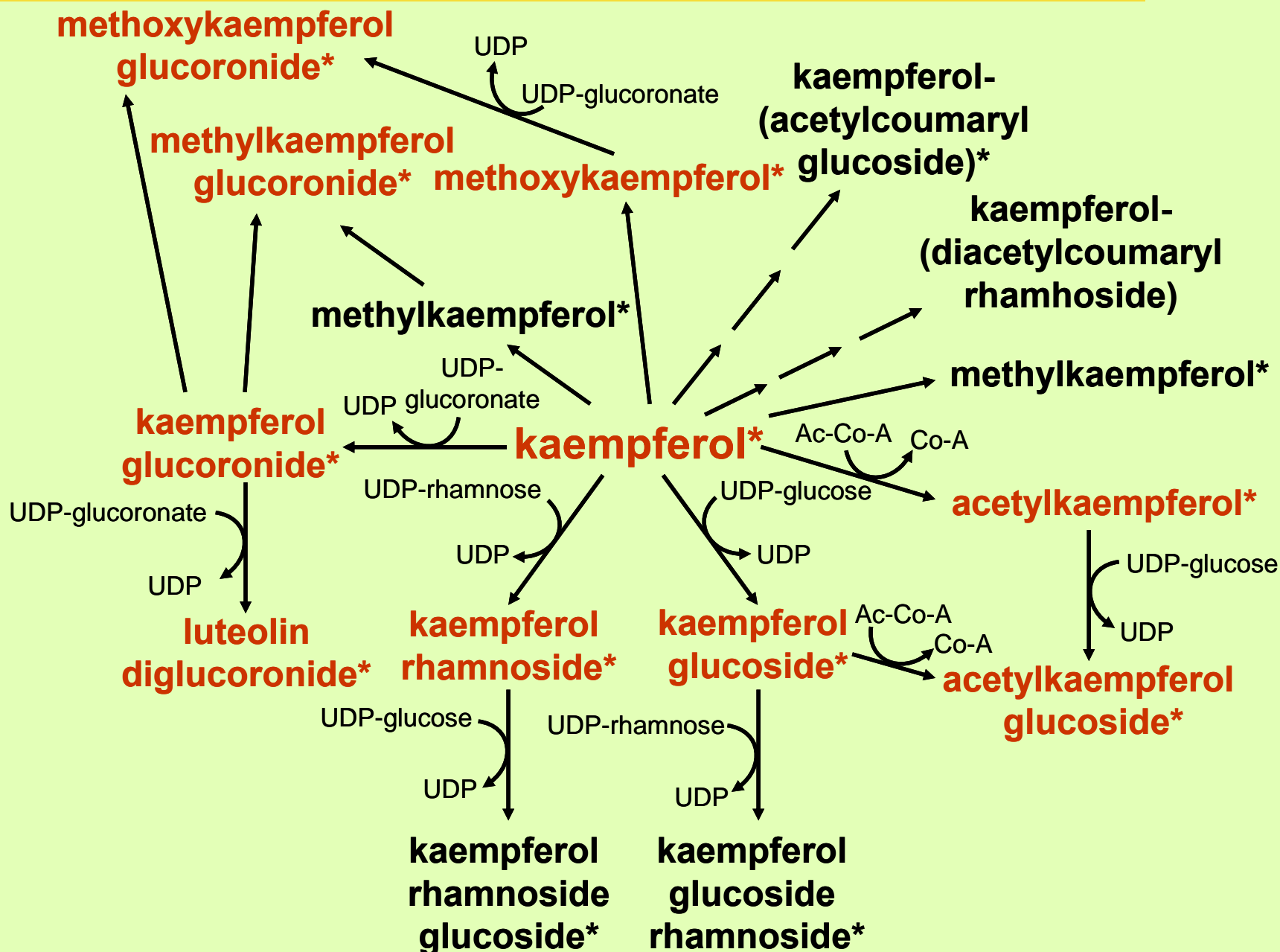
Ions analyzed by mass spec



m/z 449.10 distribution



Metabolic pathways



Conclusions: chemical imaging

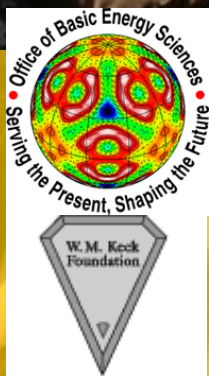
- AP MALDI
 - Peptide mixture samples: up to 3 kDa, PEG 570-630
 - Pulsed dynamic focusing for 5× signal gain → 3 fmol/pixel LOD
 - Positive and negative ions → >50 metabolites
 - MS/MS for structure identification
 - Molecular imaging of plant tissue
 - Metabolic pathways and transpiration experiment
- LAESI
 - High mass capabilities: proteins up to 66 kDa, PEG 1500
 - 8 fmol LOD
 - Quantitation: four-decade dynamic range
 - MS/MS for structure identification
 - Secondary metabolites in variegated plants
 - LAESI molecular imaging of plant tissue
 - 3D chemical imaging demonstrated
- AP IR-MALDI and LAESI are complementary



THE GEORGE
WASHINGTON
UNIVERSITY
WASHINGTON DC



Funding:
DOE – BES
NSF
W. M. Keck Foundation
GWU - REF



Acknowledgements

Discussions:
A. Vogel
L. Zhigilei

